

Influence of sulfur on the adhesion of the nickel/alumina interface

W. Zhang,¹ J. R. Smith,² X.-G. Wang,² and A. G. Evans³

¹Princeton Materials Institute, Princeton University, Princeton, New Jersey 08540, USA

²Delphi Research Labs, Shelby Twp., Michigan 48315, USA

³University of California, Santa Barbara, California 93106, USA

(Received 11 February 2003; published 27 June 2003)

The effects of sulfur on the adhesion of Ni/Al₂O₃ interfaces are determined from first principles. The interfacial bonding is analyzed in terms of its ionic, covalent, and metallic components as well as its local electron orbital symmetries. The results reveal that S segregates to intact Ni/Al₂O₃ interfaces unless those interfaces are Al rich. In all cases, the segregated S weakens interfacial bonds. The effect of S on adhesion arises from a competition between interfacial strain and new S-containing bonds formed across the interface. Results of this competition depend on whether the S is substitutional or interstitial as well as on interfacial stoichiometry. The propensity for segregation and weakening depends on the interfacial stoichiometry: governed by whether the interface is prepared by diffusion bonding or is thermally grown.

DOI: 10.1103/PhysRevB.67.245414

PACS number(s): 68.35.Gy, 68.35.Ct, 82.65.+r

I. INTRODUCTION

Certain high-temperature Ni-based alloys depend on a thermally grown Al₂O₃ layer for oxidation and corrosion protection.¹⁻⁹ Applications include hot section turbine components for power generation and aircraft propulsion,²⁻⁴ as well as automotive catalytic converter supports.⁹ To be effective, these oxide layers must remain adherent upon thermal cycling. In practice, some of the impurities in the alloy segregate to the interface, weaken the adhesion, and cause spalling:²⁻¹¹ sulfur is especially deleterious. While there has been substantial research on the adhesion of the Ni/Al₂O₃ interface,¹⁻²³ several fundamental issues have yet to be resolved. Some research suggests that, because of the size of the S ions, it does not segregate to the interface, but instead segregates to interfacial voids and affects adhesion through a void growth mechanism.⁸ Conversely, other research suggests that S segregates to interfaces between Al₂O₃ and alloys of Ni and Fe and, once at the interface, causes embrittlement.^{4-7,10} To address these and related issues, here we present solid-state computations of the energies needed to segregate S to the Ni/Al₂O₃ interface and Ni surface. We also provide computations of the effects of S on Ni/Al₂O₃ adhesion. Unless otherwise stated, calculations are performed with 1/3 monolayer (ML) at the interface.

To identify the salient challenges, the article is organized in accordance with the following topics.

(i) A discussion of the general methodology, including an approach that may be used to simulate an interface with a lattice-constant mismatch.

(ii) A model of impurity segregation, followed by details of *ab initio* computations.

(iii) Results for the S segregation to the Ni/Al₂O₃ interface and the corresponding effects on adhesion.

II. METHODOLOGY

A. Simulation of an interface with mismatch

For Ni/Al₂O₃, the mismatch between the surfaces of Ni(111) and Al₂O₃(0001) is 9.48%. A relatively large super-

cell would allow misfit dislocations to form²⁴ as in experimental interfaces. But even a cell as large as [Ni(111) × (2283 × 2283)/Al₂O₃(0001)(2500 × 2500)] still has a small misfit of 0.025%, and a cell this large is beyond the capability of current *ab initio* methods. The alternative strategy is to compute results for a variety of in-plane strains that span the range of conceivable local atomic environments¹⁵ found in experimental interfaces, consistent with the alternating regions of local stretching and contraction of the metal lattice needed to satisfy bonding across an interface with mismatch.²⁴⁻²⁸ The situation is illustrated by an unrelaxed Ni(111)/Al₂O₃(0001) interface (Fig. 1). Only the atomic layers closest to the interface are shown for clarity. Note that, in the two areas circled, the Ni atoms are above either the

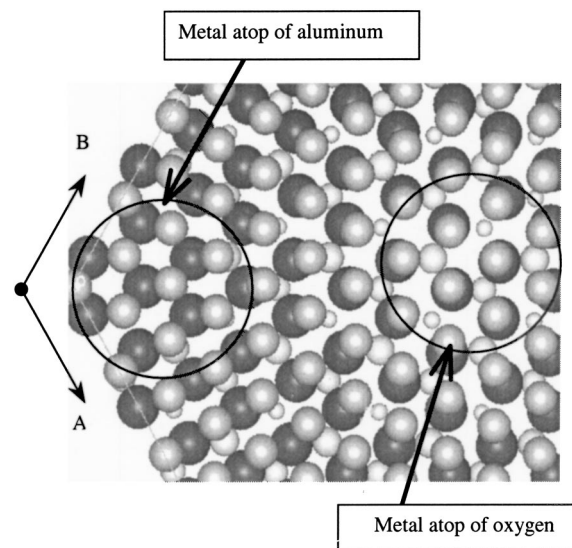


FIG. 1. View of the atomic layers closest to the interface of an unrelaxed Ni(111)/Al₂O₃(0001) interface. The lattice axes A and B are shown. The lattice C is perpendicular to the interface plane. The largest light gray spheres (top layer) represent the metal atoms. The darkest spheres are the oxygen ions. The smaller light gray spheres represent the Al ions.

oxygen sites (right circle) or the aluminum sites (left circle). At the former, to match the oxygen, the metal lattice experiences localized stretching that enhances the Ni/O bonding, accompanied by local contraction in neighboring areas.²⁷ To examine the effects of mismatch strain, three types of commensurate interfaces have been chosen that expand or contract the lattices into registry parallel to the interface. Each structure is fully relaxed by minimizing the Hellmann-Feynman forces (to within less than 0.01 eV/Å). For a *type-I interface* (T-I),¹⁵ the Ni layer is stretched by 9.48% to match an unstrained Al₂O₃(0001) layer. A *type-II interface* (T-II) is obtained by expanding the Ni by 4.74% while simultaneously compressing the Al₂O₃ by 4.74%. Both the T-I and T-II interfaces correspond to matching the Ni(111) ($\sqrt{3} \times \sqrt{3}$) with the Al₂O₃(0001) (1×1) cell [see Fig. 1(a) of Ref. 15]. A *type-III interface* (T-III) is formed by compressing the Ni(111) by 4.51% and rotating 30° relative to (an unstrained) Al₂O₃(0001), yielding an interface with a Ni(111) (2×2) cell matching the Al₂O₃(0001) (1×1) [see Fig. 1(b) of Ref. 15].

This strain generates a contribution to the energy that depends on the volume of the strained lattice. To assure that this (volume-dependent) term does not contribute to our computations of either the interfacial energy or the impurity segregation energy, the calculations compare the ensemble energy with that for the impurity and bulk materials, *subject to the same imposed strain, at the same volume*. The difference between the ensemble and the bulk materials then isolates the interface and the segregation energies from other contributions.

Previous results for the clean Ni/Al₂O₃ interface have indicated a variation in the interfacial energies with aluminum activity¹⁵ that is relatively insensitive to the procedure used to impose the strain to commensuration. This needs to be tested for impurity segregation to the interface. As discussed above, the structure of a *practical* interface with mismatch requires a relatively large unit cell containing a corresponding array of atomic configurations, whereas a matched interface has a relatively small interfacial unit cell. As the interface structure varies from site to site, the heat of segregation is site dependent. To fully understand impurity segregation, all potential impurity sites for the structures of different strains would have to be investigated. This is beyond the scope of the present study. Here, for tractability, we restrict our investigation to the three commensurate interfaces above and assert that, if the impurity does not segregate to any these interfaces, segregation is unlikely at the real interface.

B. Segregation model and heat of impurity segregation

A simple model exemplifies the definition of the heat of impurity segregation. Initially, it is assumed that the segregated S atoms occupy Ni-substitutional sites and the substituted Ni atoms enter the Ni bulk. The interfacial impurity S emanates from the Ni bulk,^{4–10} where it occupies substitutional sites. The Gibbs energy of the interface depends on the respective free energies of the Ni and S atoms located on bulk lattice sites g_{Ni}^B and g_{S}^B and those located on lattice sites at the interface, g_{Ni}^I and g_{S}^I , such that

$$G = N_{\text{Ni}}^B g_{\text{Ni}}^B + N_{\text{S}}^B g_{\text{S}}^B + N_{\text{Ni}}^I g_{\text{Ni}}^I + N_{\text{S}}^I g_{\text{S}}^I - kT \ln \Omega, \quad (1)$$

where N_{Ni}^B , N_{S}^B , N_{Ni}^I , and N_{S}^I are the corresponding numbers of atoms in the bulk and at the interface, with k the Boltzmann constant and T the temperature. The last term $-kT \ln \Omega$ describes the configurational entropy.^{29,30} The atomic structure of the Al₂O₃ side of the interface is assumed unchanged by the segregation within the model, which will be shown in Sec. III to be a reasonable approximation. For a fixed number of lattice sites, upon requiring that the total Gibbs energy be a minimum with respect to the distribution of atoms in the bulk and at the interface, and by assuming an equilibrium impurity distribution,

$$\Theta_I / (1 - \Theta_I) = \Theta_B / (1 - \Theta_B) \exp(\Delta G_{\text{seg}} / kT), \quad (2)$$

with

$$\Delta G_{\text{seg}} = -[(g_{\text{Ni}}^B + g_{\text{S}}^I) - (g_{\text{S}}^B + g_{\text{Ni}}^I)] = \Delta H_{\text{seg}} - T \Delta S_{\text{seg}}.$$

This result is the Langmuir-McLean equation describing interfacial segregation.^{29,30} In this formula, $\Theta_I = N_{\text{S}}^I / N^I$ is the S fractional occupancy of the interface, $\Theta_B = N_{\text{S}}^B / N^B$ is the S fractional occupancy of the metal bulk, ΔG_{seg} is the heat of interfacial segregation, ΔH_{seg} is the segregation enthalpy, and ΔS_{seg} is the segregation-related entropy change (excluding the configurational entropy).³⁰ The temperature dependence of ΔH_{seg} is surmised to be small and comparable to the vibrational contribution to impurity segregation at a metal grain boundary.³¹ The ΔS_{seg} is primarily determined by vibrational entropy ΔS_v (Refs. 29 and 30) and again considered to be similar to that for impurity segregation to a metal grain boundary, $-3k < \Delta S_v < 3k$ (Ref. 30). Because these temperature effects are small, we neglect all temperature-dependent terms and base our assessments on the total energy difference between the initial (before segregation) and final (after segregation) states at 0 K.

Since the interface is assumed to be in contact with a bulk Ni reservoir that contains dilute impurity S atoms at substitutional sites (Fig. 2),³² the heat of segregation can be expressed by [Eq. (2)]

$$\begin{aligned} \Delta G_{\text{seg}} = & \text{total energy of a S-free Ni/Al}_2\text{O}_3 \text{ interface} \\ & + (\text{energy of S in bulk Ni}) \\ & - (\text{total energy of the interface with S}) \\ & - (\text{energy of any extra Ni atoms entering} \\ & \text{bulk Ni}). \end{aligned} \quad (3)$$

In the following, the energies of the four parts in Eq. (3) are calculated separately. Note that the chemical potential of the S is not required for the computation of the heat of segregation: contrasting with earlier studies^{15,16} of the effects of stoichiometry, which required knowledge of the chemical potentials of the constituents. Once the heat of segregation has been determined, the equilibrium interfacial coverage of the impurity can be determined as a function of the bulk S density and temperature by means of Eq. (2).

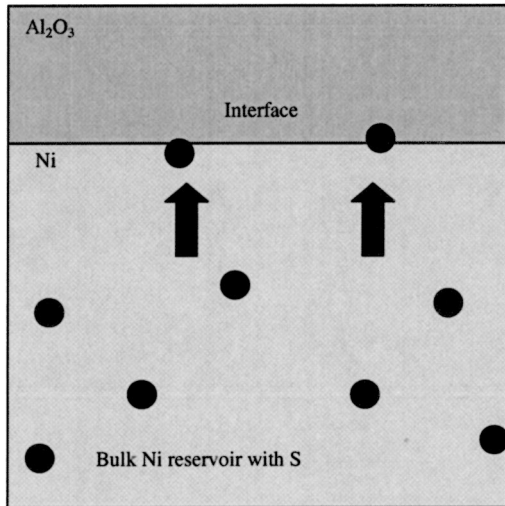


FIG. 2. Schematic model of impurity segregation at Ni/Al₂O₃ interface. The black points represent dilute impurity atoms in the metal reservoir in contact with the interface.

C. Computational method

The ensuing calculations are performed using a sandwich configuration (see Fig. 3 of Ref. 17), with alumina between two metal slabs. Each metal slab has four atomic layers, and the alumina has four O layers and eight Al layers. Periodicity is invoked parallel to the interface, and a supercell approach is employed by including a vacuum of 8–9 Å between adjacent slabs in the direction perpendicular to the interface.³³ Preliminary calculations performed using four and five atomic layers of the metal reveal differences in heats of segregation smaller than 0.1 eV/atom. All of the following results correspond to a four-layer metal slab. The Ni(111)/Al₂O₃(0001) interfacial orientation to be used^{15–17} is based on transmission electron microscopy (TEM) measurements for a similar Cu/Al₂O₃ interface.²²

First-principles computations were performed via the Vienna *ab initio* simulation program (VASP) (Ref. 34) for spin-polarized electronic structures and total energies, together with optimized ultrasoft pseudopotentials^{35,36} and the generalized gradient approximation³⁷ (GGA) for the exchange-correlation potential. Extensive tests have shown the effectiveness of the VASP package, a plane-wave electronic structure calculation program.^{15,34,36,38,39} In particular, refer to Ref. 15 for a comparison of surface and interfacial results for Ni, Cu, and Al₂O₃ systems obtained from the full-potential linearized augmented plane-wave and VASP techniques. Applications of ultrasoft pseudopotentials to the clean (Ni,Cu)/Al₂O₃ interface¹⁵ and to the sulfides of transition metals³⁸ have demonstrated their use in treating the localized Ni *d* states, as well as oxygen and sulfur states, by using a high-energy cutoff $E_{\text{cut}} = 400$ eV for the plane-wave basis set. Test calculations performed using a more exact projector-augmented-wave (PAW) method^{40,39} reveal the same trends (Table I). All calculations use the same unit-cell dimensions, energy cutoff, and a $3 \times 3 \times 1$ uniform **k**-point sampling for integrals over the Brillouin zone.

TABLE I. Comparison of heats of S segregation (eV/atom) to the Ni surface and Ni/Al₂O₃ interface. Here UP signifies ultrasoft pseudopotential, and PAW, GGA, and LDA signify the projector-augmented-wave method, the generalized gradient approximation, and the local density approximation, respectively. Adsorbed S refers to S sites above the Ni surface atoms. A surface coverage of 1/3 ML has been assumed.

System		Heat of segregation (eV/atom)		
		UP-GGA	PAW-GGA	PAW-LDA
Ni surface	Adsorbed S	2.35	2.33	2.35
	Substitutional S	1.46	1.45	1.48
Strained Ni surface	Adsorbed S	2.43	2.29	2.10
	Substitutional S	1.18	1.28	0.90
Ni/Al ₂ O ₃ interface (type I)	Al termination			
	Interstitial S	1.05	0.86	0.95
	Substitutional S	0.97	0.88	0.94
	O termination			
	Substitutional S	0.97	1.05	0.80

Prior studies of impurity-free metal/Al₂O₃ interfaces^{16,17} revealed that both the GGA and local density approximation⁴¹ (LDA) gave essentially the same stability. Here the corresponding tendencies for impurity segregation are examined. For this purpose, we considered a strain-free Ni surface and a surface stretched to match Al₂O₃(0001) (denoted T-I), as well as various interfaces (Table I). The LDA and GGA calculations were both performed using the VASP package. Based on these results (Table I), we surmise that the variation of the heat of interfacial segregation is 0.1–0.2 eV/atom (10%–20%), similar to that found for the surface energies.^{17,42}

Next, we investigate the effect of strain on S segregation to the Ni(111) surfaces. The S is initially in a ground-state substitutional site in a bulk Ni reservoir. Two different surface sites are considered: (a) substitutional in the surface atomic layer and (b) adsorbed on top of the surface at an fcc site. Strained Ni surfaces were also investigated. The results for S at the adsorption site (the site observed experimentally⁴³) are found to be relatively insensitive to strain (Fig. 3). Larger effects are found for S located on the interstitial site. The magnitudes are consistent with available experimental data^{44,45} for the heat of surface segregation (Fig. 3), as well as with data^{46,47} for the distance between the adsorbed S and top Ni plane (Table II).

III. INTERFACE SEGREGATION

A. Site occupancy of S and the heat of interface segregation

Three types of interfaces have been considered: a stoichiometric interface Ni/(Al₂O₃)_{Al}, an oxygen-rich interface Ni/(Al₂O₃)_O, and an Al-rich interface Ni/(Al₂O₃)_{Al2}. The stability of these interfaces depends on the local Al activity¹⁵ or (if there is thermodynamic equilibrium between the interface and the ambient) on the oxygen partial pressure. For each stoichiometry, results have been obtained for the three

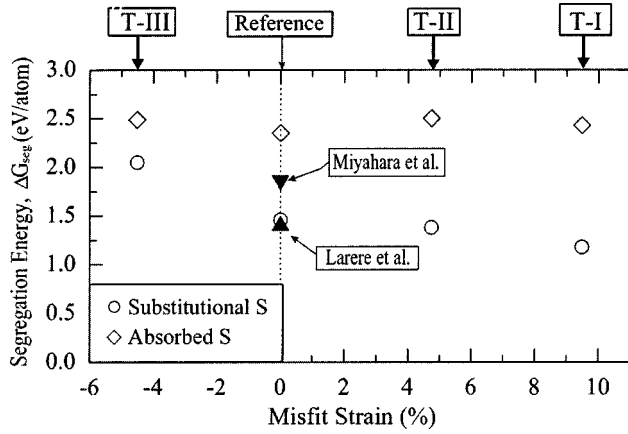


FIG. 3. Heats of segregation of sulfur to Ni(111) surfaces as a function of strain. The solid triangles are experimental data (Refs. 44 and 45).

strains T-I, T-II, and T-III. Moreover, we repeated the computations at all possible interfacial sites (Fig. 4): Ni-substitutional (S_S^{Ni}), O-substitutional (S_S^{O}), interstitial hollow (S_I^{H}), and interstitial aluminum sites (S_I^{Al}). In each case, all atomic positions were fully relaxed.

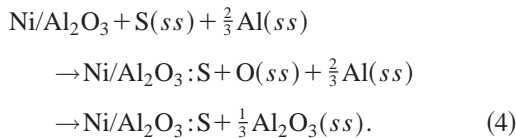
For the S_S^{Ni} site, the substituted Ni enters the Ni reservoir. When S substitutes for an O atom on the Al_2O_3 side of the interface, there are four possibilities.

(a) The extra O enters the Ni bulk (superscript O-1 in Table III), as an interstitial impurity.

(b) The O remains at the interface, but diffuses to sites close to the segregated S (high S coverage O-3). Note that the S and displaced O share the same interface unit cell in this case.

(c) The O remains at the interface but diffuses to sites remote from the segregated S (low S coverage, O-2).

(d) The substituted O atom meets a solute Al in the Ni bulk and forms Al_2O_3 (Ref. 2) in accordance with the reaction (O-4 in Table III)



where *ss* refers to a solid solution with Ni.

The effects of strain are summarized in Fig. 5. Significant effects are evident for some interfaces, especially some of

TABLE II. Distance (in Å) between S and top Ni atomic plane for Ni(111) surfaces with S at an fcc adsorption site.

Interatomic spacing $d_{\text{S-Ni}}$ (Å)		
Free	Type I	Type II
1.57	1.43	1.66
1.40 ^a		
1.60 ^b		

^aReference 46.

^bReference 47.

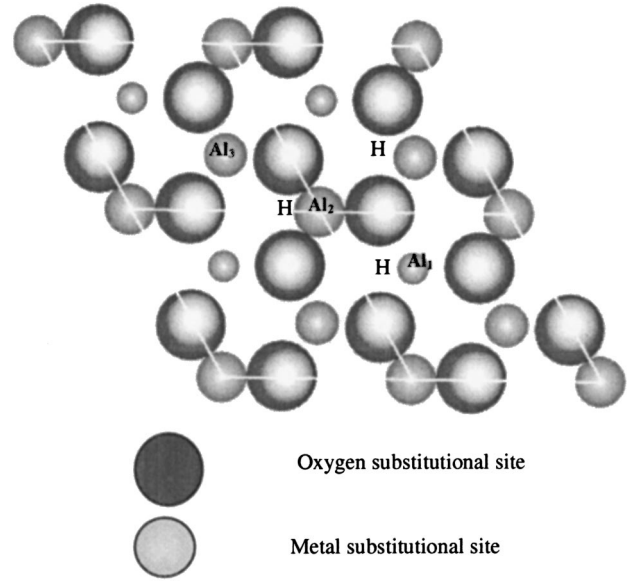


FIG. 4. Top view of a Ni/ Al_2O_3 interface and possible S occupancies. For clarity, we only show the metal layer and the Al_2O_3 (0001) layer closest to the interface. The largest gray spheres (in the top layer) represent the metal atoms. The black spheres are the oxygen ions. The smaller gray spheres represent the Al ions with three labels: those in the plane closest to the metal layer are labeled as Al_1 , while those in the plane further from the metal are labeled by Al_2 and Al_3 . *H* in the figure refers to a threefold-oxygen hollow site.

those involving interstitial S. However, the interfaces with interstitial S which show a relatively large strain effect have a negative heat of S segregation (Fig. 5): i.e., S will not segregate to them. The results for substitutional S, which are much less strain sensitive, will be used for most of the following assessment. For these cases, the segregation energies for the T-II and T-III interfaces are essentially the same. There are significant deviations when large misfit strains are used (the T-I interface). Nevertheless, the strain effects appear to be sufficiently small for the results to embody the primary trends.

Inspection of the results summarized in Table III indicates that the substitution of O by S at the interface does not occur, because the S is more weakly bonded to its neighbors than O, consistent with the relative heats of formation (HOF) of oxides and sulfides.⁴⁸ The HOF of Al_2O_3 (1675.7 kJ/mol) is more than 2 times higher than that of Al_2S_3 (724.0 kJ/mol); moreover, NiO also has much higher HOF (208.74 kJ/mol) than NiS (82 kJ/mol). The energy needed for S to segregate to the Al- or O-terminated interfaces from the bulk is lower than that for segregation to the Ni surface (see Fig. 3), presumably because the interfacial environment is more “bulk like.” This tendency is consistent with the finding that ΔG_{seg} for S segregation to a Ni grain boundary (0.98 eV/atom) (Ref. 45) is much less than that for surface segregation. We did not consider the case of the substituted oxygen atom entering the Al_2O_3 bulk because of the relatively high Al_2O_3 defect formation energy.⁴⁹ Comparing Fig. 3 with Fig. 5, note that S prefers to occupy an interstitial site on a free Ni

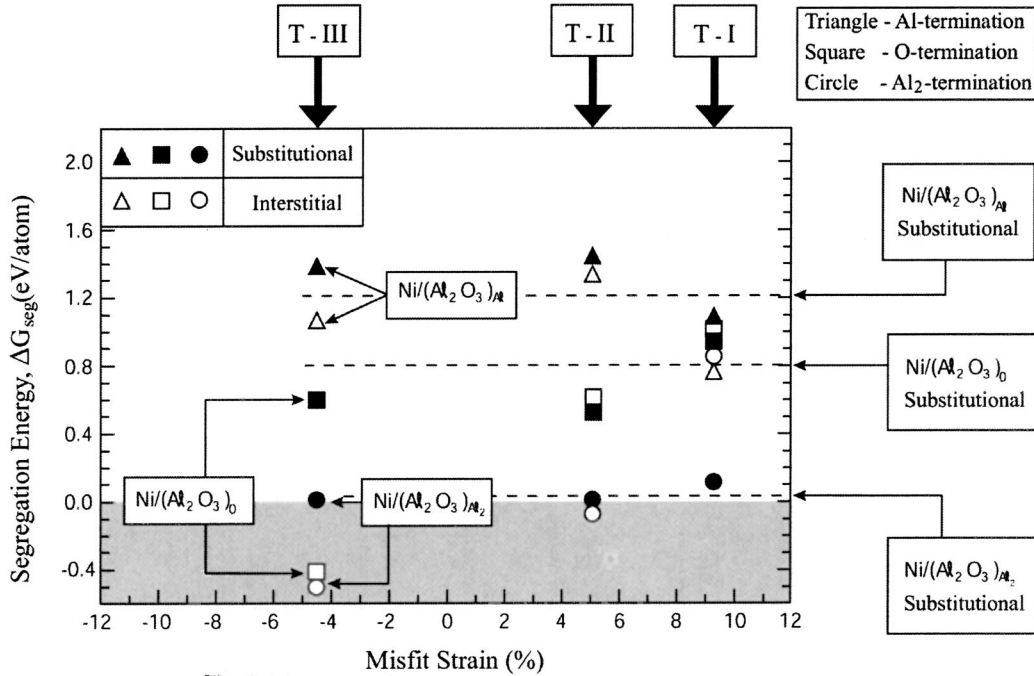


FIG. 5. Heats of segregation of S to Ni/Al₂O₃ interfaces as a function of strain in the metal parallel to the interface. Interface stoichiometry is indicated. Results for interstitial and substitutional S are given.

TABLE III. Heats of sulfur segregation ΔG_{seg} (eV/atom) from bulk Ni to the T-I Ni/Al₂O₃ interface: S_I^H refers to an interstitial hollow site, S_S^{Ni} to a Ni-substitutional site, and S_S^{O} to an oxygen-substitutional site. Negative ΔG_{seg} signifies no impurity segregation. An interfacial coverage of 1/3 ML is assumed. Energies of solute O or/and Al atoms in Ni bulk are estimated based on Ref. 50 in order to compute heats of segregation for the O-1 and O-4 cases.

System		ΔG_{seg} (eV/atom)
Ni/(Al ₂ O ₃) _{Al}	S_I^H	1.05
	$S_S^{\text{O}-1}$	-2.42
	$S_S^{\text{O}-2}$	-2.12
	$S_S^{\text{O}-3}$	-2.05
	S_S^{Ni}	0.97
	Ni/(Al ₂ O ₃) _{Al₂}	$S_I^{\text{Al}3}$
$S_S^{\text{O}-1}$		-4.65
$S_S^{\text{O}-2}$		-3.64
$S_S^{\text{O}-3}$		-2.64
$S_S^{\text{O}-4}$		+0.78
S_S^{Ni}		0.13
Ni/(Al ₂ O ₃) _O	S_I^H	0.75
	$S_S^{\text{O}-1}$	-1.49
	$S_S^{\text{O}-2}$	-1.30
	$S_S^{\text{O}-3}$	-1.09
	S_S^{Ni}	0.97

surface (adsorption site), while the Ni-substitutional site is preferred at the interface, presumably due to a difference in strain effects between the free surface and the interface (Sec. IV).

B. Work of separation

Information related to the work of separation, W_{sep} , has been determined in two ways.

(a) Obtain W_{sep} , from the surface energies σ_i and the interfacial energy γ_I as

$$W_{\text{sep}} = \sigma_1(\text{Ni side}) + \sigma_2(\text{Al}_2\text{O}_3 \text{ side}) - \gamma_I. \quad (5)$$

(b) Derive the change in the work of separation due to impurity segregation ΔW_{sep} from the heats of segregation:¹³

$$\Delta W_{\text{sep}} = (\Delta G_I - \Delta G_S)/A, \quad (6)$$

where ΔG_S is the heat of segregation to the free Ni surface, ΔG_I is the heat of segregation to the interface, and A is the cross-sectional area. The results obtained by both methods (Table IV) are consistent.

Note that, absent segregation, the O-rich Ni/(Al₂O₃)_O interface is the strongest and the stoichiometric Ni/(Al₂O₃)_{Al} interface is the weakest, consistent with measurements.^{2-4,15} The strength of the Ni/(Al₂O₃)_O interface is so large, as discussed in the next section, (as well as in Ref. 15), that a lower W_{sep} arises when 1/3 atomic layer of Ni remains attached to the (Al₂O₃)_O surface, denoted as Ni/Ni(Al₂O₃)_O. Even this lower W_{sep} is large enough to be comparable to that of bulk Ni. In every case, when S segregation occurs, it

TABLE IV. Work of separation W_{sep} (J/m^2) before and after S segregation. The ΔG_{seg} can be read from Table III and Figs. 3 and 5. A is the cross-sectional area of the interfacial unit cell.

System		Clean interface		S-segregated interface				
		W_{sep}	W_{sep}	S_S^{Ni}		S_I		
				ΔW_{sep}	$(\Delta G_I - \Delta G_S)$	W_{sep}	ΔW_{sep}	$(\Delta G_I - \Delta G_S)$
					A			A
Type I	Ni/(Al ₂ O ₃) _{Al}	1.30	1.12	-0.18	-0.17	0.17	-1.13	-1.13
		1.17 ^a						
		1.11 ^b						
	Ni(Al ₂ O ₃) _O	6.84	6.65	-0.19	-0.17	5.49	-1.35	-1.24
	Ni/Ni(Al ₂ O ₃) _O	3.25	1.97	-1.28		2.42	-0.83	
	Ni/(Al ₂ O ₃) _{Al2}	3.78	2.92	-0.86	-0.86	2.46	-1.32	-1.32
	Al ₂ O ₃ /Al ₂ O ₃	3.60						
	3.78 ^c							
	3.90 ^d							
	Ni/Ni	3.57						
Type II	Ni/(Al ₂ O ₃) _{Al}	1.12	1.10	-0.02	-0.02	0.05	-1.07	-1.07
	Ni/(Al ₂ O ₃) _O	6.54	5.76	-0.78	-0.83	4.81	-1.73	-1.73
	Ni/Ni(Al ₂ O ₃) _O	3.48	1.44	-2.04		2.17	-1.31	
	Ni(Al ₂ O ₃) _{Al2}	4.04	—			—		
	Al ₂ O ₃ /Al ₂ O ₃	4.65						
	Ni/Ni	3.75						
Type III	Ni/(Al ₂ O ₃) _{Al}	1.09	0.53	-0.56	-0.55	0.0	-1.09	-1.16
	Ni/(Al ₂ O ₃) _O	6.74	5.52	-1.22	-1.22	—		
	Ni/Ni(Al ₂ O ₃) _O	3.20	2.10	-1.10		—		
	Ni/(Al ₂ O ₃) _{Al2}	3.63	—			—		
	Al ₂ O ₃ /Al ₂ O ₃	3.60						
	Ni/Ni	3.58						

^aReference 19.

^bReference 20.

^cReference 51.

^dReference 18.

lowers W_{sep} ($\Delta W_{\text{sep}} < 0$). Moreover, after interface separation, the S remains on the Ni surface, as ascertained experimentally.^{3-7,10}

IV. INTERFACIAL STRUCTURE AND CHEMICAL BONDING

A. Clean interfaces

The atomic structures of the Al-terminated and O-terminated Ni/Al₂O₃ interfaces are shown in Figs. 6 and 7), respectively. The total, self-consistent electron density distribution for the Al-terminated interface [Fig. 8(a)] reveals the expected metallic bonding between the Ni atoms, as well as the metallic-covalent-ionic interaction between the Ni and O atoms, and the relaxed interfacial atomic structure is shown in Fig. 6(c). More instructive is Fig. 9(a) which is a

plot of the difference between the self-consistent electron density distributions and the overlapping atomic electron densities within the boxed area of Fig. 8(a), which contains the primary adhesive interaction. The dashed contours of the difference plot indicate the electron density depletion, while the solid contours indicate the electron density accumulation. Note that there is an ionic component to the Ni/Al₂O₃ bonding [Fig. 9(a)], with d electrons and s - p electrons being transferred from the Ni atoms. Moreover, the O atoms accumulate electrons that emanate from the Ni atoms as well as the Al atoms from the Al₂O₃. However, sorting out these electron transfers quantitatively is made difficult by the atom location changes (Table Va), which inhibit subtraction of free surface (self-consistent) electron densities from interfacial electron densities. Additionally, wave function overlap makes electron transfer ambiguous. Because this interface is stoichiometric, the Ni atoms bonding with the O atoms must com-

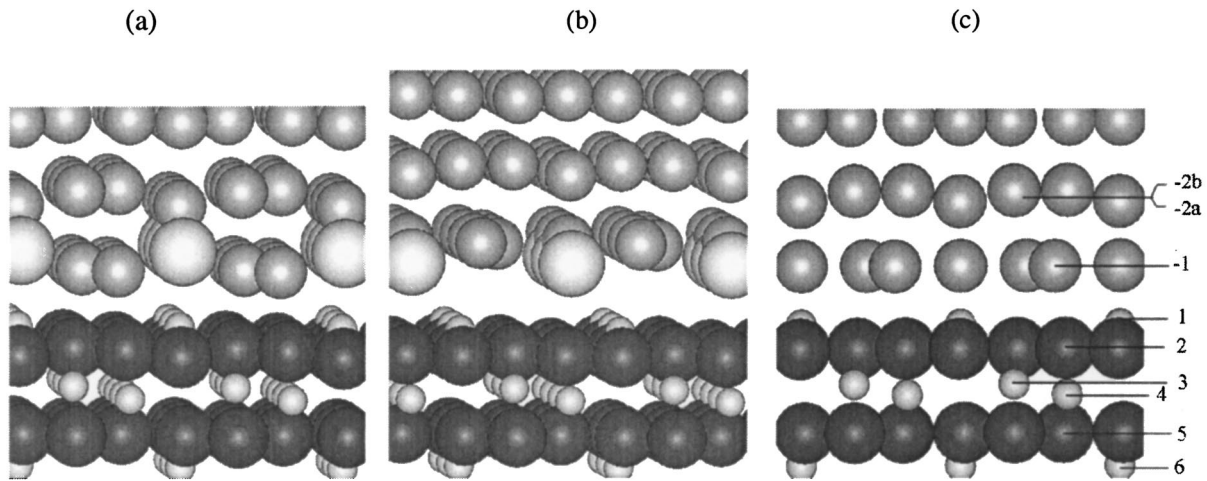


FIG. 6. Structure of the Al-terminated Ni/Al₂O₃ T-I interfaces with/without the segregated impurity S. (a) S at the Ni-substitutional sites. (b) S at the interstitial sites. (c) Clean interface. The Ni atoms are represented by the larger gray spheres, the oxygen ions by the black spheres, and the aluminum ions by the smaller gray spheres. The largest gray spheres are the S atoms.

pete with a stoichiometric compliment of Al atoms in the interface, which is presumably why the Ni/(Al₂O₃)_{Al} W_{sep} value is smaller than that for the O-terminated interface.

The total electron density contours for the O-terminated interface [Figs. 10(a) and 10(b)] again reveal the metallic bonding between Ni atoms, as well as a metallic-covalent-ionic component to the bond between the Ni and O atoms. The electrons transferred from and to the Ni orbitals [Fig. 9(b)] indicate a significant ionic contribution to the Ni-O bonding. It is also apparent that the bonding includes significant O 2*p* and Ni 3*d* contributions. Since the alumina is not stoichiometric in this interface, the Ni atoms substitute for missing Al atoms, leading to the relatively large W_{sep} . Moreover, because the Ni atoms of layer 1 [Fig. 7(c)] displace toward the O layer, the lowest W_{sep} is obtained when 1/3

monolayer of Ni atoms remain attached to the Al₂O₃ surface, denoted as Ni/Ni(Al₂O₃)_O in Table IV.

B. Segregated interfaces

1. Ni/S/(Al₂O₃)_{Al} interface

When S is located at the interstitial site [Fig. 8(b)], there is no evidence of bonds between the interfacial S and O atoms. The interstitial S is displaced away from the top oxygen layer due, in part, to the repulsive interaction between their negatively charged states at the interface. These displacements weaken the interaction between the Al₂O₃ and the Ni. When the S is substitutional, the S atom is again displaced away from the O, but now the Ni atoms in the first

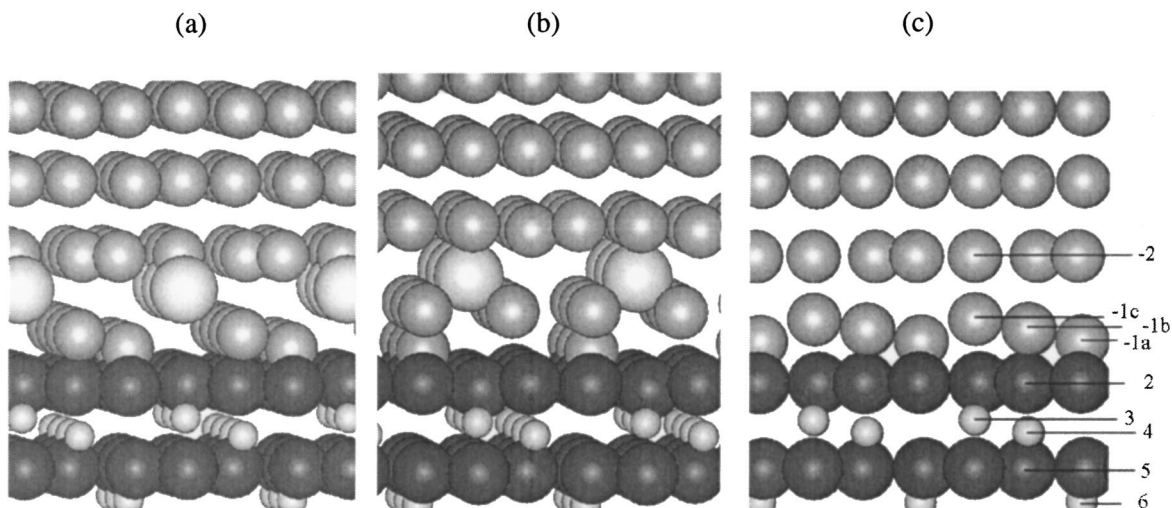


FIG. 7. Structure of the O-terminated Ni/Al₂O₃ T-I interfaces with/without the segregated impurity S. (a) S at the Ni-substitutional sites. (b) S at the interstitial sites. (c) Clean interface. The Ni atoms are represented by the larger gray spheres, the oxygen ions by the black spheres, and the aluminum ions by the smaller gray spheres. The largest gray spheres are the S atoms.

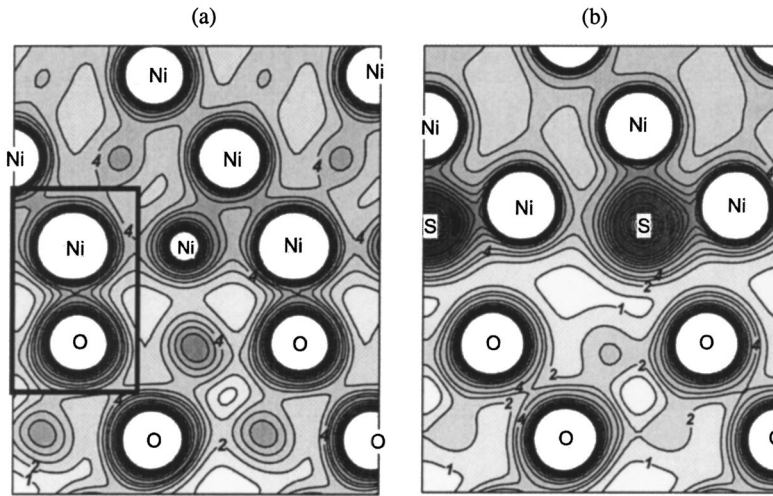


FIG. 8. Total electron charge density contour plot of $(10\bar{1}0)$ plane through interfacial oxygen and Ni atoms for the Al-terminated interface. (a) Clean interface. (b) Interface with S at an interstitial site. Note that the interstitial S atoms shift interface Ni atoms away from top of oxygen atoms and diminish the interfacial bonds between O and Ni atoms apparent in (a). The unit of the charge density is $5 \times 10^{-2} \text{ eV/\text{Å}^3}$.

TABLE V. Interfacial spacing (in Å) for the Al- and O-terminated interfaces with and without the interstitial/substitutional impurity S and comparison with bulk values. See Fig. 6 (Al-terminated) and Fig. 7 (O-terminated) for layer labeling schemes.

		Clean interface		S at interstitial site		S at substitutional site	
		Spacing	Bulk differential (%)	Spacing	Bulk differential (%)	Spacing	Bulk differential (%)
(a) Al-terminated interface							
(-2b, -2a)						0.416	—
(-2a, S)						1.117	—
(S, -1)						0.512	—
(-2, -1)	1.860	—		2.02	—		
(-1, 1)	1.512	—				1.489	—
(-1, S)				0.381	—		
(S, 1)				2.181	—		
(1, 2)	0.616	-26.75		0.412	-50.97	0.599	-28.72
(2, 3)	0.916	8.93		0.894	6.28	0.904	7.47
(3, 4)	0.280	-42.32		0.276	-43.15	0.286	-41.09
(4, 5)	0.977	16.19		0.988	17.50	0.960	14.17
(5, 6)	0.865	2.87		0.854	1.56	0.850	1.09
(b) O-terminated interface							
(-2, S)				1.287	—	0.870	—
(-2, -1c)	1.630	—					
(S, -1c)				0.802	—		
(S, -1b)						1.145	—
(-1c, -1b)	0.254	—		0.023	—		
(-1b, -1a)	0.302	—		1.037	—	0.390	—
(-1a, 2)	1.079	—		0.841	—	0.947	—
(2, 3)	0.959	14.05		0.936	11.35	0.846	0.61
(3, 4)	0.314	-35.32		0.288	-40.67	0.450	-7.30
(4, 5)	0.933	10.96		0.957	13.81	0.857	1.92
(5, 6)	0.853	1.44		0.853	1.44	0.837	-0.05

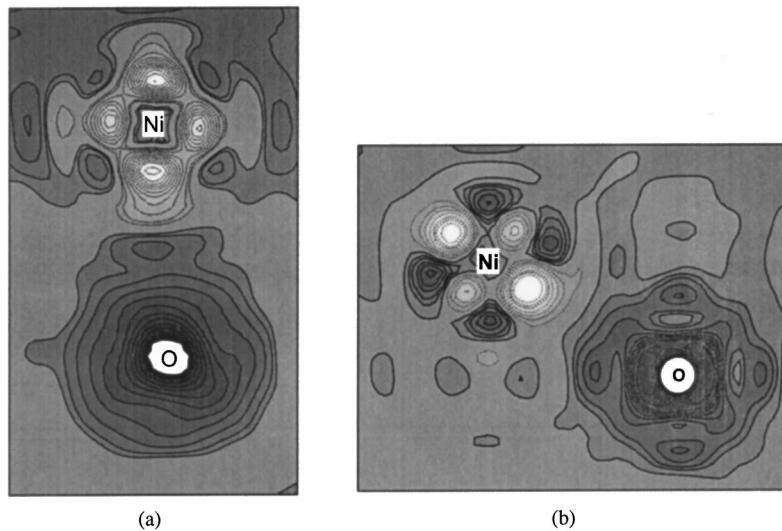


FIG. 9. Electron charge density difference contour plots. (a) Boxed area of Fig. 8(a). (b) Boxed area of Fig. 10(a). The dark gray area with solid lines indicates electron accumulation, and the light gray area with dashed lines indicates electron depletion. This plot represents the difference between the self-consistent electron density distribution of the solid interface and the sum of the overlapping atomic density distributions.

metal layer can displace closer to the $(\text{Al}_2\text{O}_3)_{\text{Al}}$ (Table V and Fig. 6(a)), resulting in a O-Ni interaction similar to that for impurity-free cases [Fig. 8(a)]. This interaction may compensate for the loss of the Ni/ Al_2O_3 interaction when S substitutes for Ni, perhaps explaining why the adhesion is similar to that for the clean interface.

2. Ni/S/ $(\text{Al}_2\text{O}_3)_\text{O}$ interface

The repulsion between the S and O atoms [Figs. 7(a), 7(b), and 10(c)] displaces the S atoms dramatically, relocat-

ing them between Ni atomic layers 1 and 2 [Figs. 7(a)–7(c)]. In consequence, the first layer of Ni atoms displace toward the $(\text{Al}_2\text{O}_3)_\text{O}$ slab, tending to saturate the oxygen dangling bonds (Table Vb). As for the clean interface, strong metallic-covalent bonding still exists between these first-layer Ni atoms and the top oxygen atoms, causing the lowest W_{sep} to occur when 1/3 ML resides on the $(\text{Al}_2\text{O}_3)_\text{O}$ surface⁵² (Fig. 7). Nevertheless, the work of separation indicates that significant chemical bonding is retained at the interface, albeit weaker than that of bulk Ni. Comparing the electron density distribution with and without S [Figs. 10(b) and

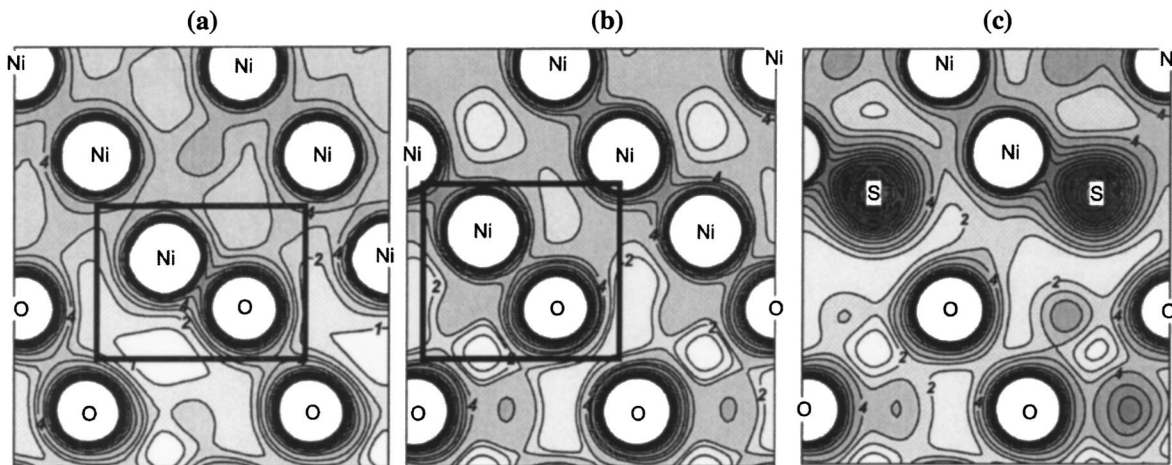


FIG. 10. Total electron charge density contours for the O-terminated interface plotted for the $(10\bar{1}0)$ plane through the interfacial O and, in the case of the clean interface, interfacial Ni atoms. (a) Clean interface with the plane through a top-layer oxygen atom and Ni atoms of plane $-1a$ [see Fig. 7(c)]. (b) Clean interface with the plane through a top-layer oxygen atom and Ni atoms of plane $-1c$ [see Fig. 7(c)]. (c) Interface with S at a Ni-substitutional site (S substitution for Ni atoms of plane $-1c$ [Fig. 7(a)]). For (c) the $(10\bar{1}0)$ plane is through the interfacial O and S and does not pass through the two Ni atomic layers closest to the O layer. The charge density has the units $5 \times 10^{-2} \text{ eV}/\text{\AA}^3$. The interfacial O-Ni bond within the box in (b) has the same characteristics as that in (a). Darker areas with lines labeled by larger numbers refer to increasing electron densities.

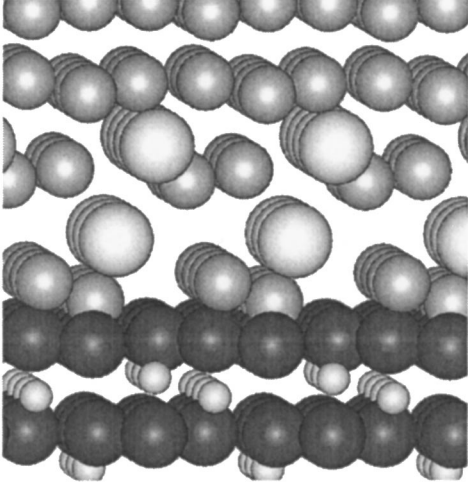


FIG. 11. Structure of the T-I O-terminated Ni/Al₂O₃ interface with 2/3 coverage of S (two S atoms per cell) segregating to Ni-substitutional sites in the interface. The large light gray spheres are S atoms.

10(c)] indicates that S substitution for Ni at the interface replaces a strong O-Ni bond by a weak S-O bond. There are also newly created S-Ni bonds closer to the (Al₂O₃)_O surface [Fig. 7(a)], which are not shown in Fig. 10(c) because they fall outside of the plane on which the contours are drawn. Although these bonds hold the interface together, they are not strong enough to counteract the lowering of the interface adhesion by the S-O bonds.

The influence of S on adhesion can be rationalized in terms of the competition between the new bonds created across the interface, involving the impurity atoms, and the weakening of the intrinsic bonds by the strain needed to accommodate the impurity,^{13,14} manifest as a larger interfacial separation. This separation is taken to be the distance $d(-2,2)$ between the oxygen layer closest to the interface and the second Ni layer (Figs. 6 and 7 and Table V). In this way, the displacement of the Ni slab relative to the Al₂O₃ slab due to S segregation can be monitored. Using this defi-

inition, the strain effect is larger when S atoms occupy an interstitial site than a substitutional site. Specifically, for the T-I Al-terminated interface [with $d(-2,2) = 3.99$ Å for the clean interface], the separation increases by 0.60 Å in the presence of interstitial S. The corresponding result for the O-terminated interface is 0.73 Å. Conversely, when S is at the Ni-substitutional site, the separation of the T-I Al-terminated interface increases by only 0.14 Å. In this case, the decrease in adhesion is mainly due to the newly formed bonds between S and its neighboring atoms not being strong enough to compensate for the loss of the Ni bonds of the substituted atom.

C. Higher S interfacial coverage

Inserting two or three substitutional S atoms into each Ni(111)/Al₂O₃(0001) (1×1) cell gives 2/3 and 1 ML coverage of interfacial S, respectively. After an extensive search of possible interfacial configurations, we found that the most stable corresponds to the second S occupying a new site in the Ni. The structure of the O-terminated interface (Fig. 11) is an example. The average heats of segregation and W_{sep} calculated for the Al-terminated and O-terminated interfaces are listed in Table VI. Note that the heat of segregation is always positive for the O-terminated interface. The ΔG_{seg} for 2/3 ML S coverage at both the Al-terminated and O-terminated interfaces decrease relative to 1/3 ML, presumably due to the strong repulsive interactions between S atoms as well as to the strain due to the relatively large S diameter. Placing the third S atom in the same Ni layer containing the second S leads to a very large interface separation and a low work of separation (zero for the Al-terminated interface and 0.62 J/m² for the O-terminated interface). Even when the third S is located in a different Ni layer, the work of interfacial separation is still much lower than that for the 1/3 and 2/3 ML cases. Furthermore, W_{sep} for the O-terminated interfaces with more than 2/3 ML S and higher coverages is now even lower relative to that for bulk Ni and Al₂O₃ (Table IV).

V. CONCLUDING REMARKS

First-principles computations have been carried out for clean and S-contaminated Ni/Al₂O₃ interfaces. The bonding

TABLE VI. Average heats of segregation (eV/atom) for 1/3 ML and higher interfacial coverages of S at Ni-substitutional (S_S^{Ni}) sites for both T-I Al-terminated (Al term) and T-I O-terminated (O term) Ni/Al₂O₃ interfaces. While the first S atom per surface unit cell occupies the Ni-substitutional site as shown in Figs. 6 and 7, the second S atom is found to occupy a different Ni layer. 3/3-II means the third S is at the second Ni layer from the interface, and 3/3-III means that the third S occupies the third Ni layer from the interface. Works of separation (J/m²) of the interfaces with impurities are also given in the table.

S coverage	Energies			
	ΔG_{seg} (eV/atom)		W_{sep} (J/m ²)	
	Al termination	O termination	Al termination	O termination
Clean			1.30	3.25
1/3	0.97	0.97	1.12	1.97
2/3	0.69	0.55	<0	1.62
3/3-III	0.62	0.61	<0	0.84
3/3-II	-0.10	0.35		0.62

of the clean Ni/Al₂O₃ interface involves not only the O 2*p* and Ni *sp* electrons, but depends significantly on Ni 3*d*-electron contributions: whereupon Ni forms relatively strong bonds with O across the interface. This is a relatively complex bond, containing ionic, metallic, and covalent aspects. When S segregates to this interface, new bonds are created, other bonds are weakened, and strains are introduced. The S and O tend to repel, and S forms a weak bond with Ni. There is a competition between the weakening effect of the interfacial strain upon S segregation and the new bonds formed across the interface. Results of this competition vary between interstitial and substitutional S and between stoichiometric (Al-terminated) and O-rich O-terminated interfaces. In all cases, when S segregates it lowers the work of separation, implying that the strain increase dominates the effects of S-induced bonds.

The calculations reveal that clean Ni/Al₂O₃ interfaces are oxygen rich and do not fail. Instead, failure occurs in one of the adjoining materials. Interfaces formed by thermal oxidation depend on the Al content in bulk Ni. For Ni (1% Al), the interface is predicted to be stoichiometric with a work of

separation significantly lower than that for either Al₂O₃ or Ni. In general, S segregates to intact Ni/Al₂O₃ interfaces, unless they are Al rich. The (already weak) stoichiometric interfaces are further weakened by such segregation. The segregation of 1/3 ML S to oxygen-rich interfaces lowers the work of separation from over 3.2 J/m² to under 2.1 J/m², consistent with experimental observations of interfacial embrittlement and spalling upon segregation.^{2,11}

If voids or cavities exist in the interface, S segregation would promote their growth because it lowers the Ni surface free energy to a greater extent than the Ni/Al₂O₃ interfacial energy. Accordingly, this study affirms that both of the proposed mechanisms of S degradation of Ni/Al₂O₃ interfaces are viable. In practice, other factors dictate the preference for one mechanism over the other.

ACKNOWLEDGMENTS

We are grateful for ONR support under Grant No. N00014-99-1-0170 and to Dr. J. L. Smialek for useful comments.

-
- ¹ *Metal-Ceramic Interfaces*, edited by M. Ruhle, A. G. Evans, M. F. Ashby, and J. R. Hirth (Pergamon, Oxford, 1990).
- ² A. G. Evans, D. R. Mumm, J. W. Hutchinson, G. H. Meier, and F. S. Pettit, *Prog. Mater. Sci.* **46**, 505 (2001).
- ³ A. G. Evans, J. W. Hutchinson, and Y. Wei, *Acta Mater.* **47**, 4093 (1999).
- ⁴ F. G. Gaudette, S. Suresh, and A. G. Evans, *Metall. Mater. Trans. A* **31**, 1977 (2000).
- ⁵ J. L. Smialek, *JOM* **52**, 22 (2000); *Metall. Trans. A* **22**, 739 (1991).
- ⁶ J. L. Smialek, *Thin Solid Films* **253**, 285 (1994).
- ⁷ P. Y. Hou, *Mater. Corros.* **51**, 329 (2000); P. Y. Hou and J. L. Smialek, *Mater. High Temp.* **17**, 79 (2000); P. Y. Hou and J. Stringer, *Oxid. Met.* **38**, 323 (1992).
- ⁸ H. J. Grabke, G. Kurbatov, and H. J. Schmutzler, *Oxid. Met.* **43**, 97 (1995); H. J. Grabke, D. Wiemer, and H. Viehhaus, *Appl. Surf. Sci.* **47**, 243 (1991).
- ⁹ R. Sigler, *Oxid. Met.* **40**, 555 (1993).
- ¹⁰ J. D. Kiely, T. Yeh, and D. A. Bonnell, *Surf. Sci. Lett.* **393**, L126 (1997).
- ¹¹ S. Addepalli, N. P. Magtoto, and J. A. Kelber, *Langmuir* **16**, 8352 (2000).
- ¹² S. Y. Hong and A. B. Anderson, *Surf. Sci.* **230**, 175 (1990).
- ¹³ J. R. Smith and T. V. Cianciolo, *Surf. Sci. Lett.* **210**, L229 (1989); X.-G. Wang, J. R. Smith, and A. E. Evans, *Phys. Rev. Lett.* **89**, 286102 (2002). T. Hong, J. R. Smith, and D. J. Srolovitz, *Phys. Rev. B* **47**, 13 615 (1993); W. Zhang and J. R. Smith, *Phys. Rev. Lett.* **82**, 3105 (1999).
- ¹⁴ T. Hong, J. R. Smith, and D. J. Srolovitz, *Acta Metall. Mater.* **43**, 2721 (1995).
- ¹⁵ W. Zhang, J. R. Smith, and A. G. Evans, *Acta Mater.* **50**, 3803 (2002).
- ¹⁶ W. Zhang and J. R. Smith, *Phys. Rev. Lett.* **85**, 3225 (2000); *Phys. Rev. B* **61**, 16 883 (2000).
- ¹⁷ J. R. Smith and W. Zhang, *Acta Mater.* **48**, 4395 (2000).
- ¹⁸ I. G. Batirev, A. Alavi, and M. W. Finnis, *Phys. Rev. Lett.* **82**, 1510 (1999).
- ¹⁹ E. Saiz, R. M. Cannon, and A. P. Tomsia, *Acta Mater.* **47**, 4209 (1999).
- ²⁰ D. Chatain, L. Coudurier, and N. Eustathopoulos, *Rev. Phys. Appl.* **23**, 1955 (1988).
- ²¹ V. Merlin and N. Eustathopoulos, *J. Mater. Sci.* **30**, 3619 (1995).
- ²² G. Dehm, M. Ruhle, D. Ding, and R. Raj, *Philos. Mag. B* **71**, 1111 (1995).
- ²³ J. Schnitker and D. J. Srolovitz, *Modell. Simul. Mater. Sci. Eng.* **6**, 153 (1998).
- ²⁴ R. Benedek, A. Alavi, D. N. Seidman, L. H. Yang, D. A. Muller, and C. Woodward, *Phys. Rev. Lett.* **84**, 3362 (2000).
- ²⁵ F. C. Frank and J. H. Van Der Merwe, *Proc. R. Soc. London, Ser. A* **198**, 205 (1949).
- ²⁶ C. Scheu, G. Dehm, M. Ruhle, and R. Brydson, *Philos. Mag. B* **78**, 439 (1998).
- ²⁷ R. Benedek, D. N. Seidman, and C. Woodward, *J. Phys.: Condens. Matter* **14**, 2877 (2002).
- ²⁸ I. Vilfan, T. Deutsch, F. Lancon, and G. Renaud, *Surf. Sci. Lett.* **505**, L215 (2002).
- ²⁹ E. D. Hondros and M. P. Seah, *Metall. Trans. A* **8**, 1363 (1977); E. D. Hondros, M. P. Seah, S. Hofmann, and P. Lejcek, in *Physical Metallurgy*, edited by R. W. Cahn and P. Hassen (Elsevier Science BV, Amsterdam, 1996), Chap. 13.
- ³⁰ S. Hofmann, in *Surface Segregation Phenomena*, edited by P. A. Dowben and A. Miller (CRC Press, Boca Raton, 1990), Chap. 4.
- ³¹ J. Creuze, F. Berthier, R. Tétot, B. Legrand, and G. Tréglia, *Phys. Rev. B* **61**, 14 470 (2000).
- ³² In bulk Ni free of strain, a S atom has a somewhat lower total energy (0.15 eV) in a substitutional site than it does in an interstitial site in VASP GGA calculations. Substitutional S is assumed throughout our computation for all cases.

- ³³M. C. Payne, M. P. Teter, D. C. Allan, T. A. Arias, and J. D. Joannopoulos, *Rev. Mod. Phys.* **64**, 1045 (1992).
- ³⁴G. Kresse and J. Hafner, *Phys. Rev. B* **47**, R558 (1993); G. Kresse and J. Furthmüller, *ibid.* **54**, 11 169 (1996).
- ³⁵D. Vanderbilt, *Phys. Rev. B* **41**, 7892 (1990).
- ³⁶G. Kresse and J. Hafner, *J. Phys.: Condens. Matter* **6**, 8245 (1994).
- ³⁷J. P. Perdew, in *Electronic Structure of Solids '91*, edited by P. Ziesche and H. Eschrig (Akademie Verlag, Berlin, 1991), p. 11.
- ³⁸P. Raybaud, G. Kresse, J. Hafner, and H. Toulhoat, *J. Phys.: Condens. Matter* **9**, 11 085 (1997); **9**, 11 107 (1997).
- ³⁹G. Kresse and D. Joubert, *Phys. Rev. B* **59**, 1758 (1999).
- ⁴⁰P. E. Blöchl, *Phys. Rev. B* **50**, 17 953 (1994).
- ⁴¹J. P. Perdew and A. Zunger, *Phys. Rev. B* **23**, 5048 (1981).
- ⁴²J. P. Perdew, J. A. Chevary, S. H. Vosko, K. A. Jackson, M. R. Pederson, D. J. Singh, and C. Fiolhais, *Phys. Rev. B* **46**, 6671 (1992).
- ⁴³*Adsorption on Metal Surfaces*, edited by J. Benard (Elsevier Scientific, Amsterdam, 1983).
- ⁴⁴T. Miyahara, K. Stolt, D. A. Reed, and H. K. Birnbaum, *Scr. Metall.* **19**, 117 (1985).
- ⁴⁵A. Larere, M. Guttman, D. Dumoulin, and C. Roques-carnes, *Acta Mater.* **39**, 685 (1982).
- ⁴⁶J. E. Demuth, D. W. Jepsen, and P. M. Marcus, *Phys. Rev. Lett.* **32**, 1182 (1974).
- ⁴⁷M. Zharnikov, M. Weinelt, P. Zebisch, M. Stichler, and H.-P. Steinrück, *Phys. Rev. Lett.* **73**, 3548 (1994).
- ⁴⁸*CRC Handbook of Chemistry and Physics*, 78th ed., edited by D. R. Lide (CRC Press, Boca Raton, FL, 1997).
- ⁴⁹G. J. Dienes, D. O. Welch, C. R. Fischer, R. D. Hatcher, O. Lazareth, and M. Samberg, *Phys. Rev. B* **11**, 3060 (1975).
- ⁵⁰Y. A. Chang, K. Fitzner, and M.-X. Zheng, *Prog. Mater. Sci.* **32**, 97 (1988); *Selected Values of Thermodynamic Properties of Metals and Alloys*, edited by R. Hultgren, R. L. Orr, P. D. Anderson, and K. K. Kelly (Wiley, New York, 1963).
- ⁵¹K. C. Hass, W. F. Schneider, A. Curioni, and W. Andreoni, *Science* (Washington, DC, U.S.) **282**, 265 (1998).
- ⁵²For the T-I O-terminated Ni/Al₂O₃:S interfaces with S at substitutional sites, the work of separation with two Ni atoms (2/3 of the first Ni atomic layer from the interface) sticking to the Al₂O₃ surface is 1.73 J/m², somewhat lower than that with one Ni atom (1/3 of the first Ni atomic layer) sticking to the Al₂O₃ surface (1.97 J/m²) as listed in Table IV for type-I strain. To be comparable with the clean interface, we use the value of W_{sep} corresponding to the latter case.